Available online at www.sciencedirect.com
SCIENCE DIRECT®
Surface Science xxx (2005) xxx–xxx
SURFACE SCIENCE
www.elsevier.com/locate/susc

Relaxations in the 1×5 reconstruction of Pt(1 1 0)

I.K. Robinson [a,*], M.C. Saint-Lager [a], P. Dolle [b], S. Boutet [a], M. De Santis [b], R. Baudoing-Savois [b]

[a] *Department of Physics, University of Illinois, 1110 West Green St., Urbana, IL 61801, United States*
[b] *CNRS Laboratoire de Cristallographie, Grenoble, BP 166-38042 Grenoble Cedex 09 France*

Received 17 September 2004; accepted for publication 22 November 2004

Abstract

Pt(1 1 0) is one of the most closely investigated metal surface structures because it displays a variety of "missing-row" reconstructions, which are only marginally stable. The ground state is usually found to have 1×2 translational symmetry, but a 1×3 form has also been seen. Between 1×2 and 1×3, a series of disordered structures has been recorded, which shows a slight preference for 1×5 periodicity. Under the preparation conditions used in this study, a stable 1×5 structure was found for Pt(1 1 0). Investigation by surface X-ray diffraction has led to a complete three-dimensional structure, which closely resembles an alternation of 1×2 and 1×3 unit cells. Pt(1 1 0) shows an interesting example of two "homometric" structures that are indistinguishable by diffraction, but are distinguishable by virtue of their subsurface relaxation pattern.

Keywords: Missing row; Reconstruction; X-ray diffraction; Platinum

1. Introduction

The "missing row" theme of reconstruction of face-centred cubic (fcc) (1 1 0) surfaces has attracted the interest of surface science since its inception. The reconstructed surface adopts nanofacets of {1 1 1} orientation alternately arrayed to make up an overall (1 1 0) surface. This lowers the energy because {1 1 1} facets are close-packed and have a lower surface energy than {1 1 0} facets for fcc materials. This "missing row" type of reconstruction, for which some examples are shown in Fig. 1, forms spontaneously for the noble metals Au, Pt and Ir, but can be induced in less noble metals such as Cu, Ag, Pd by chemical modifications, particularly when charge transfer from an alkali metal is used [1–3]. Alloy (1 1 0) surfaces,

* Corresponding author.
E-mail address: ikr@uiuc.edu (I.K. Robinson).

0039-6028/$ - see front matter © 2004 Elsevier B.V. All rights reserved.
doi:10.1016/j.susc.2004.11.035

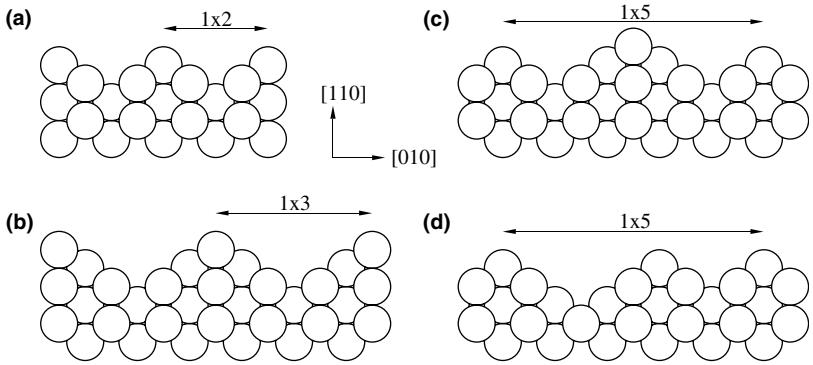

Fig. 1. Schematic side views of the missing-row structures of Pt(1 1 0) considered in this article. The surface is at the top of the picture, the bulk at the bottom. Conventional fcc crystal directions are labelled; the surface coordinate system relabels the vertical direction as [0 0 1] and the horizontal as [0 1 0]. (a) 1×2, (b) 1×3, proposed 1×5 structure in (c) "hill" variant and (d) "valley" variant.

particularly those involving these end-row transition elements, are also found to display the "missing row" reconstruction [4,5]. It can also be induced by epitaxy in thin metal films of the same elements [6].

Historically, the "missing row" reconstructions have been among the first structures to be investigated by new experimental and theoretical techniques. Important examples are the scanning tunnelling microscope by Binnig and Rohrer [7], low energy electron diffraction (LEED) [8], atomic resolution transmission electron microscopy [9] and surface X-ray diffraction [10]. Surface theoretical techniques, such as the local density approximation (LDA) and embedded atom method (EAM), have also been tested on these systems. The surface atoms within the "missing row" reconstruction have unusual coordination, which makes them a good test of theories that are generalized from the bulk. The application of LDA methods to Au(1 1 0) 1×2 [11] was an important step. Later, the induction of the reconstruction in Ag(1 1 0) was explained by LDA modelling of charge transfer [12].

It is the length scale of the nanofacetting effect to lower the surface free energy that determines whether the surface adopts the 1×2, 1×3 or indeed $1 \times n$ "missing row" structure. The lowest-order energy difference between these, obtained by counting nearest-neighbour bonds [13], is zero. Both Au(1 1 0) and Pt(1 1 0) are thus believed to be 1×2 structures in the ground state, because this is what is most commonly observed. There is a tendency for surfaces to switch between different length scales (or values of n) under the slightest influence, such as the coverage of alkali metal [3,14]. The $Pt_{80}Fe_{20}$ alloy (1 1 0) surface was found to switch between these reconstructions as a function of annealing treatment following ion bombardment, which was attributed to segregation effects seen in the structures [5]. Switching is also possible due to the effect of low concentrations of impurities and has led to reports of multiple, or ambiguous, ground state structures. In some cases this has allowed detailed investigations of the less common state, for example the Pt(1 1 0) 1×3 investigated by LEED [15] and X-ray diffraction [19] as well as an analogous Au(1 1 0) 1×3 [16].

The low energy difference between the 1×2 and 1×3 also invites the possibility of disordered states in between and beyond. Many of the known systems have phase transitions in which the long-range order is lost above a certain temperature due to statistical generation of units of another length [18]. Since unbalanced facet sizes can lead to an overall change in height of the surface, this might also be linked to surface roughening transitions [20]. A study of Pt(1 1 0) found a gradual transition from 1×2 to 1×3 took place while keeping the sample at a fixed temperature of 600 °C and this was subsequently related to the segregation of carbon at the surface over several hours [21]. Examination of the evolution of the dif-

fraction peaks and widths showed evidence for an intermediate 1×5 state that was badly ordered [21]. The present paper reports that the Pt(1 1 0) 1×5 has now been stabilized and that its three-dimensional structure has been solved by surface X-ray diffraction.

2. Experimental method

The sample was cut from a Pt single crystal and polished to $0.17 \pm 0.05°$ from the 1 1 0 plane. The UHV sample preparation was achieved by Ar^+ sputtering at 1 keV or 800 eV for 20–30 min, under conditions that gave about 6–8 μA of ion current. The sputtering was alternated three times with annealing of 5 min at 600 °C in 5×10^{-7} mbar oxygen gas. After a final sputtering the sample was annealed in UHV for 5 min at 750 °C to give a sharp RHEED pattern showing the 1×5 reconstruction. Auger spectroscopy at this stage showed no carbon contamination within the 0.1 ML sensitivity of our spectrometer. At the end of the experiment at a base pressure of 2×10^{-10} mbar, a small carbon peak was observed, equivalent to about 0.15 monolayers of carbon, which was probably present all along, but not detected immediately after the preparation.

In subsequent experiments, the expected 1×2 reconstruction was obtained only after annealing in oxygen, without the UHV annealing step. This behaviour is roughly consistent with the previous studies [21], carried out on a different crystal, that found signs of the 1×5 reconstruction during annealing at 600 °C. The earlier work found only a very disordered 1×5, while the present sample preparation produced a sample that was sufficiently ordered for a full diffraction data set to be collected, over a duration of several hours. The same earlier experiment ended with an ordered 1×3 surface, whose structure was determined [19], and attributed to carbon impurities detected by Auger spectrometry at a level of a fraction of a monolayer, but without calibration. It is assumed in the present study that carbon is also primarily responsible for the change of structure to 1×5, but that other (undetected) impurities might account for the difference in its level of ordering from the earlier work. STM experiments on Pt(1 1 0) and Au(1 1 0) showed a similar result, that the presence of trace impurities led to an increased density of 1×3 units on the surface [17].

The X-ray diffraction measurements were made at the BM32 bending magnet beamline of the ESRF at the dedicated 6-circle UHV diffractometer. An incidence angle of 1° was used throughout the measurements. The sample was aligned by means of two bulk Bragg reflections using the control program "spec" operating in a custom 6-circle mode. X-rays of 18 keV were used to achieve large out-of-plane momentum transfer. A tetragonal surface-based coordinate system was adopted for indexing the data so that the (1 1 0) surface normal direction was spanned by a single Miller index, L. The lattice constant along y was chosen to be five unit cells so that all rods of the reciprocal lattice could be indexed with integers. The resulting choice was $a = 2.77$ Å, $b = 19.6$ Å and $c = 2.77$ Å, pointing along the cubic crystal directions $(1\bar{1}0)$, (0 0 1) and (1 1 0) respectively.

A full crystallographic data set was measured *at room temperature* for the 1×5 structure by integration of rocking curves at 336 different positions along the superstructure and crystal truncation rods (CTRs). The width of the scans was found to be about the same for the two kinds of rod, indicating that the 1×5 superstructure was well-enough ordered that the peak widths were determined by the resolution of the detector slits. The integrated intensities were corrected for active sample area, Lorentz and polarisation factors, then averaged using p2mm symmetry. The agreement between 128 strong equivalent reflections was 8.2%, which was used to set the systematic errors on an absolute scale [22]. The resulting 172 data points, falling along the 14 superstructure rods and 2 CTRs shown as symbols in Figs. 2 and 3, were then used to fit the structure.

3. Structure determination and refinement

The known 1×2 and 1×3 "missing row" structures consist of alternating {1 1 1} nanofacets of width 2 and 3 rows respectively. The low surface

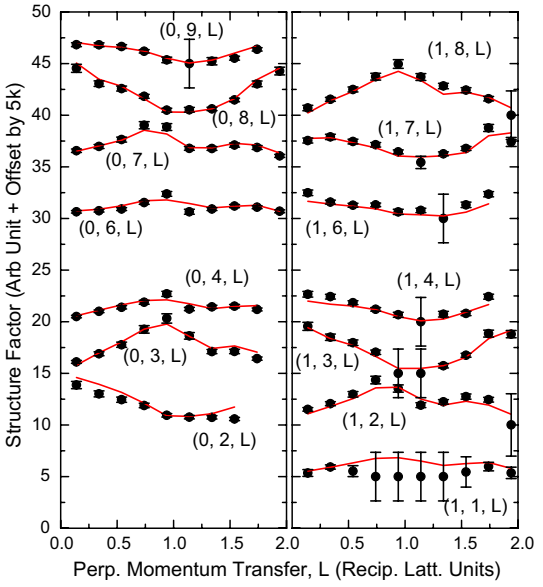

Fig. 2. X-ray diffraction measurements of the superstructure rods of the Pt(1 1 0) 1×5 structure. The curves have been offset vertically in units of 5 times the Miller index k. The best fit to the data with $\chi^2 = 2.74$ is overlaid as solid lines.

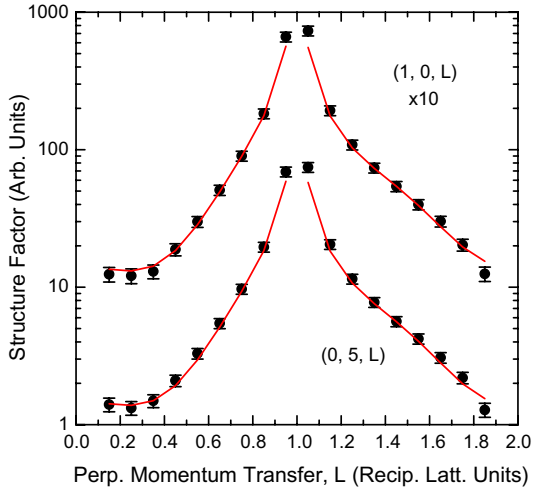

Fig. 3. X-ray diffraction measurements of the crystal truncation rods of the Pt(1 1 0) 1×5 structure. The curves have been offset vertically by a factor of 10. The best fit to the data with $\chi^2 = 2.74$ is overlaid as solid lines.

energy of this close packed facet is assumed to stabilize the structure. The 1×5 has been found previously to lie *between* the 1×2 and 1×3 structures, so is likely made up of alternations of 2-row and 3-row motifs [21]. Evaluation of all possible structures of this kind, that conserve the overall height of the surface in the long range, shows that there are just two possibilities for the 1×5 structure. These are denoted as the "hill" structure and the "valley" structure shown in Fig. 1. The potential structures with 5-row, or 4-row plus 1-row terraces can be ruled out immediately because of their very bad fits to the data, with $\chi^2 > 30$. In any case, these are considered unlikely to occur in between the 1×2 and 1×3 structures for thermodynamic reasons. Earlier STM experiments on the K-induced 1×5 structure of Au(1 1 0) appeared to support the "valley" model, with its uniform height and non-uniform spacing of the visible ridges [14].

The "hill" structure and the "valley" structure were immediately tested to see if they showed agreement with the data, using the standard surface analysis program ROD [23]. Without allowing any displacements or disorder the resulting χ^2s were found to be *identical*, with a value of 10.8, after varying roughness and scaling parameters. Given the high quality of the data, either of these represents quite good agreement. This does present a serious problem of uniqueness, because the two structures of Fig. 1(c) and (d) are clearly not the same. Why they give identical diffraction patterns is a consequence of Babinet's principle: the "holes" in one structure match exactly the atoms of the other. This structure is an example of non-uniqueness of structure which is extremely rare in crystallography, with a known example being the mineral structure of Bixbyite, which is also precisely ambiguous between two chemically different configurations of the unit cell [24,25]. Both the ideal Pt(1 1 0) 1×5 and Bixbyite are examples of "homometric" structures [26–28].

Fortunately, missing row structures tend to show strong relaxation, and the relaxed versions of the hill and valley structures cannot remain indistinguishable: a displaced "hole" cannot contribute to the structure factor while a displaced atom can. Starting at the top of each structure, atomic displacements (as defined in Fig. 4) were introduced gradually and refined against the measured data. In both cases, the agreement stopped

improving after the fifth layer was allowed to relax: the χ^2 did not drop any further and the fit started to show singular behaviour, indicating insensitivity to one or more of the parameters. Layerwise Debye–Waller (DW) factors were introduced at the same time. The resulting fits were highly reproducible from a wide range of starting configurations.

After relaxation, the ''hill'' structure reached a χ^2 of 3.91, while the ''valley'' structure reached a χ^2 of 4.76. Allowing a variable ''surface fraction'' (see below) brought the χ^2 of the ''hill'' structure down to 3.35. Both patterns of relaxation appear plausible, with reasonable interatomic spacings. On this basis we can say that we favour the ''hill'' structure but cannot exclude the ''valley'' structure outright. The earlier STM study of Pt(1 1 0) [17] detected the gradual appearance of occasional 1×3 units which exposed the third layer. While this appears to suggest the ''valley'' structure on the local scale, it is not clear that a fully ordered configuration would have the same local arrangement. Another STM study of Au(1 1 0) 1×5 induced by K deposition also indicated the ''valley'' structure was preferred [14].

We next investigate ways in which the structure might consist of some sort of ''mixture'' of the two structures. From the general point of view of disorder in diffraction, there are two fundamentally different ways of mixing structures, coherently and incoherently. A coherent mixture allows interference between the structures; the coherent limit implies that the length scale over which the structures are mixed is smaller than the coherence length of the experiment. Conversely, the incoherent limit assumes isolated regions of each structure and a superposition only of intensities, not amplitudes. For our structure, both kinds of mixture were tried and both led to an improvement of the overall χ^2.

The incoherent mixture was tested by fitting fractions of the intensity of the two refined structures, along with a common roughness and scale factor. For simplicity, the coordinates and DW factors were not refined during this procedure; the χ^2 values were lower by about 0.36 for this reason: pure ''hill'' gave $\chi^2 = 3.59$; pure ''valley'' gave $\chi^2 = 4.25$. The best fit for the incoherent mixture was with 69% ''hill'' and 31% ''valley''. This gave a $\chi^2 = 3.39$, which would correspond roughly to 3.75 if the parameters had been varied.

The coherent mixture was tested by varying the occupancy of certain sites in the refined ''hill'' model. So long as the change in occupancy is small, this represents statistical mixtures of unit cells with their extra atoms present or absent. According to Fig. 1, if the three atoms on one face of the larger 1×3 hill are removed, the structure morphs into the valley structure. To keep symmetry, the occupancy of the five atoms covering both faces of the 1×3 were varied together. Upon doing this, the occupancy dropped from 1 to 0.90 and the χ^2 dropped from 3.91 to 3.63, while continuing to refine the position parameters. An alternative way to morph the structure is to add two additional rows of atoms onto the side of the smaller 1×2 hill. Again to preserve symmetry, this was done on both sides: the four extra atoms took an occupancy of 0.10 with $\chi^2 = 3.72$. When both changes were allowed simultaneously, the first occupancy rose to 0.93, the second dropped to 0.04 and $\chi^2 = 3.60$. Based on the improvement in χ^2, we can conclude that the coherent mixture is slightly more relevant than the incoherent one and that the admixture of valley structures is roughly at the 10% level.

The CTR data in Fig. 3 were found to be particularly sensitive to the differences between the ''hill'' and ''valley'' models, with the former giving a calculated structure factor for small L that was too small and the latter one that was too large. Even the coherent mixture with $\chi^2 = 3.60$ did not give particularly good agreement on the tails of the Bragg peaks. Previously, with disordered structures, it has been found that a variable (coherent) ''surface fraction'', f_S, can account for parts of the structure that contribute to the bulk, but not to the surface [23]. Specifically, this was found to be useful in the previous study of Pt(1 1 0) 1×3 which gave $f_S = 0.89$ [19]. A way to think of this is that only a fraction of the sample bears a reconstruction while the remainder remains ''unreconstructed'' or ''1×1'', but still contributes coherently. Here, also a variable surface fraction led to a much better fit with $\chi^2 = 2.74$ and $f_S = 0.93$. Once the four insignificant parameters from the list of possible near-bulk

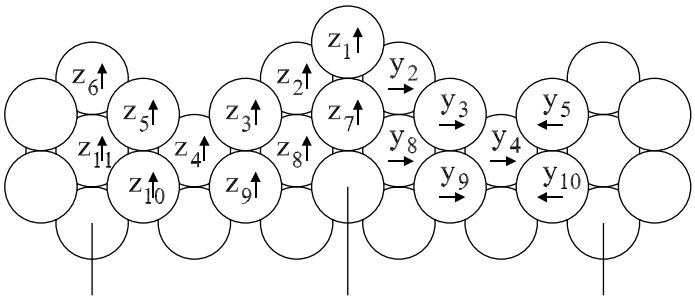

Fig. 4. Labelling scheme of the atomic displacement parameters used in the final model of the 1×5 structure. Parameter values are listed in Table 1. Mirror symmetry is assumed about the vertical tick lines, so that most atoms have both vertical and horizontal displacements.

displacements were removed, this was taken to be the final model and its parameter values are listed in Table 1 corresponding to the parameter labels of the model in Fig. 4. The first occupancy parameter mentioned above rose to 0.96, while the second increased to 0.14. The surface roughness parameter was $\beta = 0.06$. Three isotropic Debye–Waller factors were refined, $B_1 = 2.2$ Å^2 for the 1×3 ridge atom, $B_2 = 1.6$ Å^2 for the 1×2 ridge atom and $B_3 = 0.65$ Å^2 for the two second layer atoms on the 1×3 ridge. The fit curves passing through the data in Figs. 2 and 3 were obtained with this last $\chi^2 = 2.74$ model.

Table 1
Parameter values corresponding to the displacements defined in Fig 4

Parameter	Displacement (Å)
y_2	0.031(4)
y_3	0.019(4)
y_4	—
y_5	0.037(4)
y_8	—
y_9	0.011(4)
y_{10}	0.014(4)
z_1	−0.167(16)
z_2	−0.071(12)
z_3	0.045(13)
z_4	0.092(7)
z_5	0.043(13)
z_6	−0.080(13)
z_7	−0.011(13)
z_8	—
z_9	0.019(7)
z_{10}	—
z_{11}	—

Values are in Å with the uncertainty in the least significant digits in parenthesis. The quoted uncertainty is from the least-squares fit only, which ignores other sources of error and tends to overestimate the overall reliability. The limited range of data would be responsible for an overall accuracy, due to the method itself, of around ±0.01 Å parallel to the surface and ±0.02 Å perpendicular. Parameters denoted '—' were found to be unnecessary as judged by their increasing of the overall χ^2.

4. Comparison of the structure with earlier work

Having explored the disorder in the 1×5 Pt(1 1 0) structure, we now turn to the refined coordinates themselves and compare them with the individual 1×2 and 1×3 structures solved previously. The model discussed in this section is the "hill" model with a small (coherent) fraction of "valley" mixed in, together with a small fraction of unreconstructed surface, giving $\chi^2 = 2.74$ as described above. Only the coordinates of the "hill" part of this model were refined and only those were used to determine the interatomic spacings. Fig. 5 shows the interatomic spacing (bondlength) information revealed by the refined positional coordinates; deviations from the bulk spacing of 2.77 Å are shown multiplied by 100 for clarity. As expected from the earlier missing-row structures, big contractions surround the ridge rows of atoms, with the 1×3 ridge considerably more contracted than the 1×2. The {1 1 1} facets formed by the surface layer show strong lateral contractions throughout the structure, with the strongest contractions near the apex of the two ridges, especially the 1×3. Alternating regions of expansion and

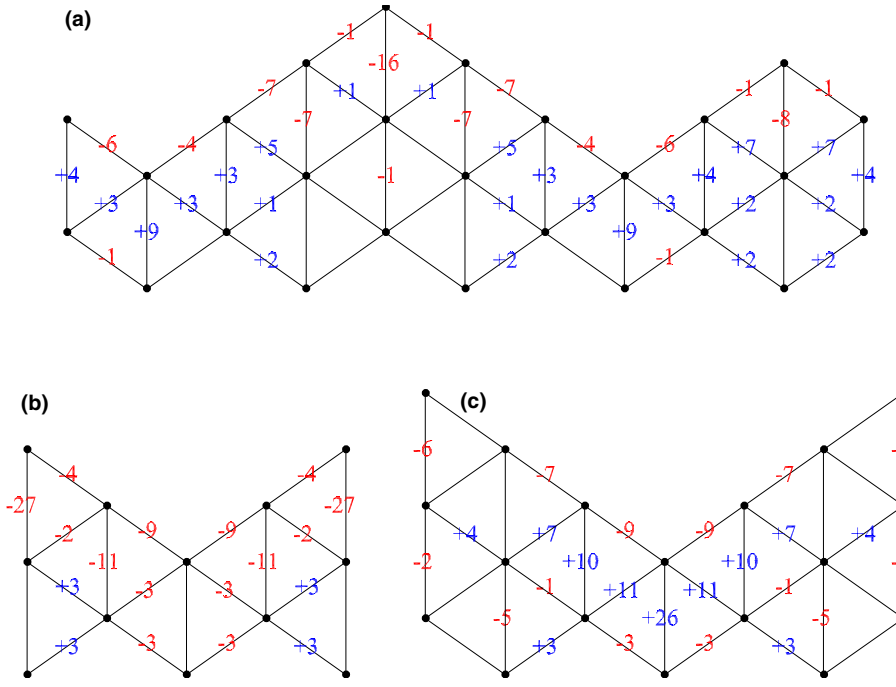

Fig. 5. (a) Deviations in the interatomic separations in the refined Pt(1 1 0) 1×5 structure from the ideal bulk separation of 2.77 Å. Values displayed are in Å units multiplied by 100. The uncertainty is typically ±2 of these units. (b) Analogous picture for the published Pt(1 1 0) 1×2 X-ray structure [34]. (c) Analogous picture for the published Pt(1 1 0) 1×3 X-ray structure [19].

contraction can be discerned in the near-bulk regions with a general contraction under the 1×3 and expansion under the 1×2. This has the general effect of "flattening" the surface, or decreasing the inclination angle of the facets in the structure.

The pattern of expansions and contractions generally reproduces that seen in the pure 1×3 structure, reproduced from the published X-ray structure [19] for comparison in Fig. 5(c). The 1×3 has relatively less contraction near the top of the ridge and more expansion near the bottom of the valley than is seen here in the 1×5. As discussed in the previous paper [19], the structures determined by low-energy electron diffraction (LEED) [15] and also by medium energy ion scattering for Cs/Au(1 1 0) 1×3 [29], both have larger contractions around the ridge than found in the X-ray structure [19]. In fact those two non X-ray results agree better with the situation found here for Pt(1 1 0) 1×5.

The environment of the atoms along the ridges of the structure is unusual and worth close attention. The ridge atoms have only seven nearest neighbours within the structure, very different from the bulk fcc coordination number of 12. It is important that theories of the solid state be able to reproduce the structure of metal atoms in this extreme and highly anisotropic configuration for our understanding of structure in general. For example, the LDA calculation for Au(1 1 0) 1×2 predicts an average contraction for the ridge atoms of 2.7% [11]. The heuristic "glue" model of Ercolessi, Tosatti and Parinello [30], also for Au, predicts a 7.8% contraction of the 7-coordinated atoms [19]. The two separate measurements here of the average contraction of the interatomic spacing around the 7-coordinated ridge atoms are 1.0% and 0.6%. In all cases, the experiments and LDA theory fall short of the glue model prediction. This could be because the "embedding" term featured by the "glue" model is not sensitive to geometry: the environment of the ridge atom is highly anisotropic with all the neighbours on one side and most of the contraction localized near the plane perpendicular to the ridge.

There are enough positional coordinates in the structure to test further some of these widely-used general concepts of the role of coordination number in metal surface structure. A very general argument originated by Smoluchowski [31] and developed for surfaces by Finnis and Heine [32] is that the shape of the electron cloud surrounding the ion cores in a metal adapts to smooth the boundaries of the electron density. One class of practical theoretical models based on this idea, that has seen widespread application to predict the properties of metal surfaces, is the ''embedded-atom'' model [33], otherwise called the ''glue'' model mentioned above [30]. This model incorporates a general assumption that there is a positive correlation between coordination, the number of nearest neighbours, and the degree of contraction seen by each atom. This allows an ''embedding'' term to be added to the energy functional which depends on coordination. Low-coordinated atoms can compensate for their lack of embedding by bringing their neighbour atoms closer, hence reducing the average interatomic spacing or bondlength.

To attempt a quantitative test of the coordination-contraction effect, we can evaluate the average bondlengths for the different atoms in the Pt(1 1 0) 1×5 structure. The two 7-coordinated sites in the unit cell (ridge rows), discussed above, have average contractions of 0.028 Å and 0.017 Å, under the 1×3 and 1×2 ridges respectively. The three independently determined 9-coordinated sites (on {1 1 1} facets) have average contractions of 0.023 Å, 0.010 Å and −0.002 Å, the last being a small expansion. The one 11-coordinated site has a net contraction of only 0.001 Å. The near-bulk region provides six independent distorted bulk sites with coordination number 12; these are found to be mostly *expanded* spacings with average expansions of: 0.006 Å, 0.013 Å, 0.004 Å, −0.011 Å, 0.013 Å and 0.023 Å. The overall trend is slightly towards expansion of the spacings rather than contraction. Interestingly, the two extreme cases are associated with the bulk atoms immediately below the two ridges, −0.011 Å below the 1×3 and 0.023 Å below the 1×2 ridge, showing completely opposite trends.

For comparison, we relate the corresponding numbers for the published Pt(1 1 0) 1×2 [34] and 1×3 X-ray structures [19] in Fig. 5(b) and (c). The 1×2 is one of the earliest structures determined using X-rays in three dimensions. Compared with the modern studies, it has very few measurement points and not very well-determined displacement parameters. Within the 1×3 structure, the 7-coordinated site has an average contraction of 0.009 Å while the two 9-coordinated sites have average contractions of 0.016 Å and 0.009 Å. The 11-coordinated site at the bottom of the valley has a large net expansion of 0.031 Å. The near-bulk region (12-coordinated) has average expansions of: 0.007 Å, 0.013 Å, 0.025 Å, 0.012 Å, −0.002 Å and −0.001 Å, with the largest expansions at the bottom of the valley [19].

In all of these examples, the trend of neighbour-contraction with lower coordination is clearly apparent, but it is by no means a strong trend, almost at the level of the scatter of the various determinations. Especially in the pure 1×3 structure, the largest overall changes are expansions rather than contractions. This suggests that other mechanisms than the Smoluchowsky smoothing may be at play, notably anharmonicity (finite temperature) and/or local charge transfer effects.

In summary, we have solved the structure of yet another variation of the ''missing-row'' reconstruction on a fcc (1 1 0) surface. Under the preparation conditions used in this study, a stable 1×5 structure was found for Pt(1 1 0). The complete three-dimensional structure closely resembles an alternation of 1×2 and 1×3 unit cells. The results show an interesting example of two ''homometric'' structures that are indistinguishable by diffraction, but are distinguishable by virtue of their different subsurface relaxation patterns.

Acknowledgments

We acknowledge fruitful discussions with Prof. John Spence of Arizona State University about the ''homometric'' properties of Bixbyite. Parts of this work were supported by the National Science Foundation under DMR 03-08660, the US Department of Energy under DEFG02-91ER45439 and the CNRS Cristallographie-University of Illinois

exchange program. The ESRF is acknowledged for the provision of beam time at BM32.

References

[1] J.W.M. Frenken, R.L. Kraus, J.F. van der Veen, E. Holub-Krappe, K. Horn, Phys. Rev. Lett. 59 (1987) 2307.
[2] C.J. Barnes, M. Lindroos, D.J. Holmes, D.A. King, Surf. Sci. 219 (1989) 143.
[3] R. Schuster, I.K. Robinson, Phys. Rev. Lett. 76 (1996) 1671.
[4] R. Koller, Y. Gauthier, C. Klein, M. De Santis, P. Varga, Surf. Sci. 530 (2003) 121.
[5] R. Baudoing-Savois, Y. Gauthier, W. Moritz, Phys. Rev. B 44 (1991) 12977.
[6] E. Platzgummer, M. Sporn, R. Koller, M. Schmid, W. Hofer, P. Varga, Surf. Sci. 453 (2000) 214.
[7] G. Binnig, H. Rohrer, Surf. Sci. 126 (1983) 236.
[8] W. Moritz, D. Wolf, Surf. Sci. 88 (1979) L29.
[9] L.D. Marks, D.J. Smith, Nature 303 (1983) 316.
[10] I.K. Robinson, Phys. Rev. Lett. 50 (1983) 1145.
[11] K.M. Ho, K.P. Bohnen, Phys. Rev. Lett. 59 (1987) 1833.
[12] C.L. Fu, K.M. Ho, Phys. Rev. Lett. 63 (1989) 1617.
[13] I. Vilfan, J. Villain, Surf. Sci. 257 (1991) 368.
[14] J.V. Barth, R. Schuster, J. Wintterlin, R.J. Behm, G. Ertl, Phys. Rev. B 51 (1995) 4402.
[15] P. Fery, W. Moritz, D. Wolf, Phys. Rev. B 38 (1988) 7275.
[16] G.A. Held, J.L. Jordan-Sweet, P.M. Horn, A. Mak, R.J. Birgeneau, Solid State Commun. 72 (1989) 37.
[17] T. Gritsch, D. Coulman, R.J. Behm, G. Ertl, Surf. Sci. 257 (1991) 297.
[18] J. Villain, I. Vilfan, Surf. Sci. 199 (1988) 165.
[19] I.K. Robinson, P.J. Eng, C. Romainczyk, K. Kern, Phys. Rev. B 47 (1993) 10700.
[20] I.K. Robinson, E. Vlieg, K. Kern, Phys. Rev. Lett. 63 (1989) 2578.
[21] I.K. Robinson, P.J. Eng, C. Romainczyk, K. Kern, Surf. Sci. 367 (1996) 105.
[22] I.K. Robinson, in: D.E. Moncton, G.S. Brown (Eds.), Handbook on Synchrotron Radiation, vol. III, Elsevier, North Holland, 1990.
[23] E. Vlieg, J. Appl. Cryst. 33 (2000) 401.
[24] W.H. Zachariasen, Z. Krist. 67 (1928) 455.
[25] L. Pauling, M.D. Shappel, Z. Krist. 75 (1930) 128.
[26] A.L. Patterson, Phys. Rev. 65 (1944) 195.
[27] M.J. Buerger, Z. Krist. 143 (1976) 79.
[28] R. Hosemann, S.N. Bagchi, Acta Cryst. 7 (1954) 237.
[29] P. Häberle, P. Fenter, T. Gustafsson, Phys. Rev. B 39 (1989) 5810.
[30] F. Ercolessi, E. Tosatti, M. Parinello, Phys. Rev. Lett. 57 (1986) 719.
[31] R. Smoluchowsky, Phys. Rev. 60 (1941) 661.
[32] M.W. Finnis, V. Heine, J. Phys. F 4 (1974) L37.
[33] K.W. Jacobsen, J.K. Norskov, M.J. Puska, Phys. Rev. B 35 (1987) 7423.
[34] E. Vlieg, I.K. Robinson, K. Kern, Surf. Sci. 233 (1990) 248.